metals

MDPI

Article

Microstructure and Fracture Behavior of Refill Friction Stir Spot Welded Joints of AA2024 Using a Novel Refill Technique

Lipeng Deng [1,2,*], Shuhan Li [1], Liming Ke [1], Jinhe Liu [2] and Jidong Kang [3]

[1] School of Aeronautical Manufacturing and Engineering, Nanchang Hangkong University, Nanchang 330063, China; shuhanli@outlook.com (S.L.); limingke@nchu.edu.cn (L.K.)
[2] School of Material Science and Engineering, Northwestern Polytechnical University, Xi'an 710072, China; jinhliu@nwpu.edu.cn
[3] Canmet MATERIALS, Natural Resources Canada, 183 Longwood Road South, Hamilton, ON L8P0A5, Canada; jidong.kang@canada.ca
* Correspondence: denglipeng@nchu.edu.cn; Tel.: +86-138-7066-5644

Received: 30 January 2019; Accepted: 27 February 2019; Published: 3 March 2019

Abstract: Keyhole at the end of a conventional friction stir welded (FSW) joint is one of the major concerns in certain applications. To address this issue, a novel keyhole refilling technique was developed for conventional friction stir spot welding (FSSW) using resistance spot welding (RSW). A three-phase secondary rectifier resistance welder was adapted for the refill of the keyhole in the 1.5 mm + 1.5 mm friction stir spot welded 2024-T4 aluminum alloy joint. The microstructure and tensile shear fracture behavior were compared for both the unfilled and refilled specimens. The results show that the plug and keyhole are dominated by solid state welding with some localized zones by fusion welding. The refill process significantly improved the maximum load capacity in tensile shear testing as the corona ring is enlarged leading to a larger bonding area. Moreover, the tensile shear fracture occurs in the refilled FSSW specimens at the corona bonding zone, while the fracture occurs at the hook zone in the unfilled keyhole.

Keywords: friction stir spot welding; resistance spot welding; keyhole; aluminum alloy

1. Introduction

Friction stir welding (FSW) is a patented welding technique developed by The Welding Institute (TWI) in 1991 [1]. As a solid-state welding process, the metallurgical properties of the weldment could be partly maintained or even be better than those of the parent material. Therefore, this technique could be applied to join materials that exhibit an adverse reaction during conventional fusion welding, such as metal matrix composites, dissimilar materials, rapidly solidified materials, etc. [2,3]. Since its inception, FSW has continuously gained practical applications in a wide range of manufacturing fields such as aerospace, automotive, ship-building, and high-speed train manufacturing.

During the FSW process, a cylindrical tool with a specially designed shoulder and a probe is typically used. The rotating tool is inserted into the workpieces and then traversed along the weld line. Heat created by friction and plastic deformation of the materials, results in softening of the workpieces. With the tool rotation and traverse movement, the workpieces are joined.

One major drawback of the FSW technique is that a keyhole remains at the end of the weld. To avoid it, several methods have been developed. These include the refilling friction stir welding (RFSW) that adopts a telescopic stir-pin for welding [4–6], which is invented by GKSS (a national research centre in Germany) at firstly, pinless or probeless friction stir spot welding [7–9], friction plug welding (FPW) [10–13], filling friction stir welding that adopts a retention pin [14], and fusion welding

filling [15]. Although these techniques could effectively eliminate the keyhole in some cases, each appears to have some restrictions in practice.

In this paper, a novel refill technique is developed for friction stir spot welding (FSSW) using resistance spot welding (RSW), which is a popular manufacturing method in aerospace and automotive industries [16,17]. To demonstrate the validity of the technique, it is first applied to refill the keyhole created through FSSW of 1.5 mm thick AA2024 aluminum sheets. A detailed comparative study was carried out with a focus on the microstructure and tensile shear fracture behavior of the unfilled and refilled friction stir spot welded joints.

2. Material and Experimental Procedures

The material used in the present study is 1.5 mm thick AA2024-T4 aluminum alloy sheets. The nominal chemical composition of the alloy is listed in Table 1.

Table 1. Nominal chemical composition of AA2024 (wt. %).

	Cu	Si	Fe	Mn	Mg	Zn	Cr	Ti	Al
AA2024	3.8–4.9	0.5	0.5	0.3–0.9	1.2–1.8	0.25	0.1	0.15	Bal.

FSSW was conducted on an in-house developed FSSW machine. The following welding parameters were used: rotational speed of 1500 r/min, plunge depth of 0.30 mm, and holding time of 20 s, which are reported by Karthikeyan R., et al. [18].

The welding machine used for refill is a three-phase secondary rectifier resistance spot welder with a power of 300 kVA, which can implement the spot welding of the 1.5 mm + 1.5 mm aluminum alloy and simultaneously load three types of welding pressures (i.e., parallel, step-like, and saddle-shaped) and a multi-pulsed current for pre-heating, welding, and slow cooling. The welding pressure is stepless adjustable from 0.5 kN to 30.0 kN and the welding current (DC) is adjustable from 3 kA to 60 kA by controlling the conduction angle of thyristors. This machine is a DC welding machine, and the upper electrode is positive pole, the lower electrode is negative pole, and it can display the welding current, electrode pressure, and thermal expansion displacement and allows the welder to perform real-time monitoring. The machine is made by the school, and is popular in aerospace manufacturing as a Hanson Welding Machine. The keyhole refilling process using RSW is illustrated in Figure 1a. The specimen alignment and welding are implemented automatically under the combined effect of the pressure from the electrodes and that of the welding current. A metallurgical joining is then formed between the plug and materials surrounding the keyhole, as shown in Figure 1b.

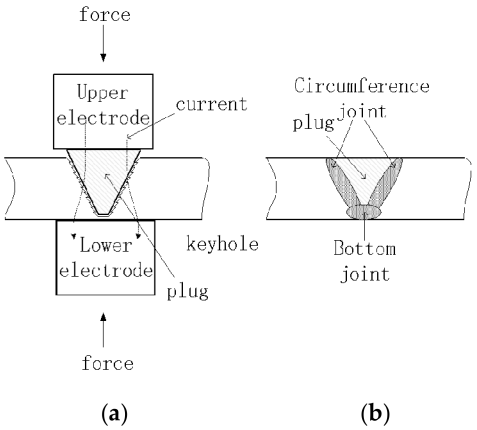

Figure 1. The illustration of the new refill technique using resistance spot welding (RSW). (**a**) unfilled; (**b**) filled.

The upper and lower electrodes are shown in Figure 2. Note that the upper electrode has a conical frustum shape with a lower base diameter greater than that of the upper portion of the keyhole. The lower electrode has a planar surface. Both the upper and lower electrodes are machined from an alumina dispersion strengthened copper bar. During the refilling process, the upper electrode pushes the plug and the weld is placed on one end of the lower electrode.

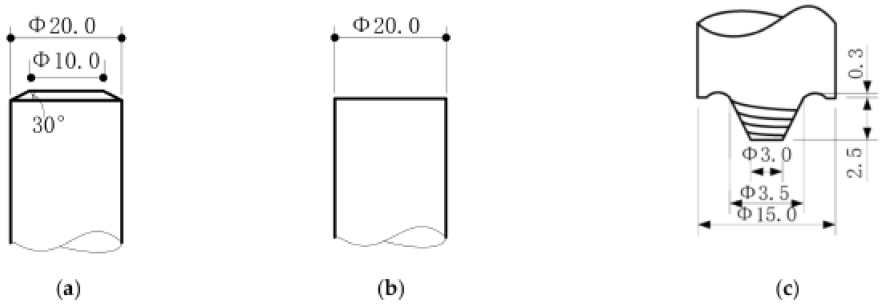

Figure 2. The sketch of the upper and lower electrode and the tool for friction stir spot welding (FSSW) (unit: mm). (**a**) upper; (**b**) lower; (**c**) tool for FSSW.

The Figure 2c is the tool for FSSW. The keyhole created in the center of the specimen after FSSW is sketched in Figure 3a. The shape of the plug is depicted in Figure 3b displaying the structure of the frustum of a cone. On the inner wall of the keyhole, there are thread turning traces of the probe, improving the contact resistance between and dispersing the current lines flowing through the plug and the keyhole. The parameters for refill are welding time of 200 ms, welding pressure of 10 kN, and welding current of 28 kA, 31 kA, 34 kA, 37 kA, and 40 kA. The parameters are all from preliminary experiments by the method of controlling single variable parameter.

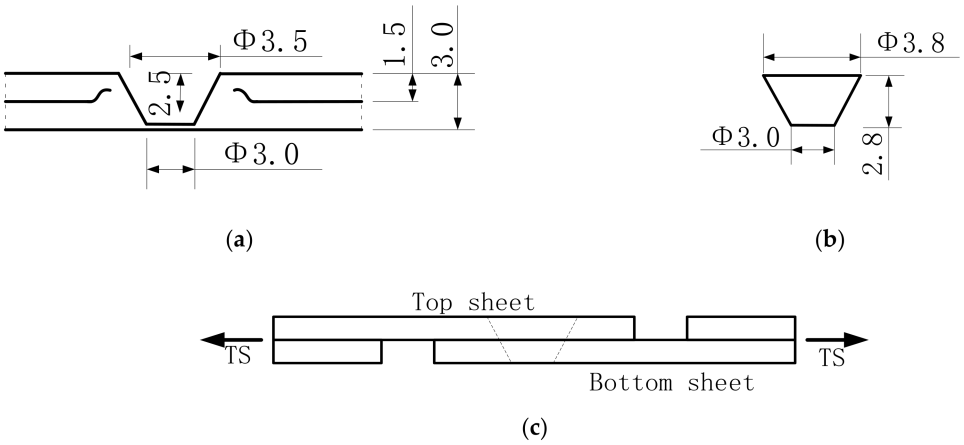

Figure 3. The dimension of keyhole and plug (unit: mm). (**a**) keyhole; (**b**) plug; (**c**) the specimens for tensile-shear (TS) test.

The tensile-shear (TS) specimens were prepared according to the dimensions shown in Figure 3c. All tensile shear tests were conducted at a speed of 1 mm/min. The load and displacement were simultaneously recorded during the testing.

In order to understand the variation in hardness between different regions of the friction stir spot welds, microhardness measurements were made on a line scan across the middle of the upper sheet with a spacing of 0.2 mm. The load used in the microhardness measurements was 200 g for a duration of 10 s.

Fractured tensile shear specimens were collected for fractography using scanning electron microscopy (SEM, FEI Company, Hillsboro, OR, USA).

3. Experimental Results and Discussion

3.1. Tensile-Shear Testing

Five FSSW specimens with refilled holes for each welding condition with different welding currents (28 kA, 31 kA, 34 kA, 37 kA, and 40 kA respectively) along with five groups FSSW with unfilled keyholes with same FSSW parameters were selected for static TS testing at room temperature. Tensile forces were plotted against cross head movement to produce the average value of maximum TS forces shown in Figure 4. The average maximum tensile shear force was calculated to be 5.45 kN for the FSSW specimens with unfilled keyholes. In the refilled FSSW specimens, the TS force first increases and then decreases with increasing welding current with a peak value of 7.25 kN at a weld current of 37 kA which is 33% higher than that of the unfilled FSSW specimens. The weld current is one of the setting parameters in the processing of filling keyhole by RSW. With the current increasing, the area of bonding is increasing between the plug and keyhole, and between the top sheet and the bottom sheet especially, the later bonding area can improve the TS force dramatically. But when the current is too high, the cracks or cavities are observed in the joint, which decrease the TS force. It was found that the local plug rapidly melted and changed into liquid metal by the larger weld current, and escaped from the keyhole remaining a few small gaps. In the crystallization process, there was not enough metal to refill the gaps, and the cracks or shrinkage cavities were formed. The standard deviation of unfilled FSSW joints' TS force is the smallest, and that of the filled joints with maximum TS force is lesser than unfilled joints, but that of the filled joints with maximum weld current is the largest. Only specimens under this welding condition were used for further analyses.

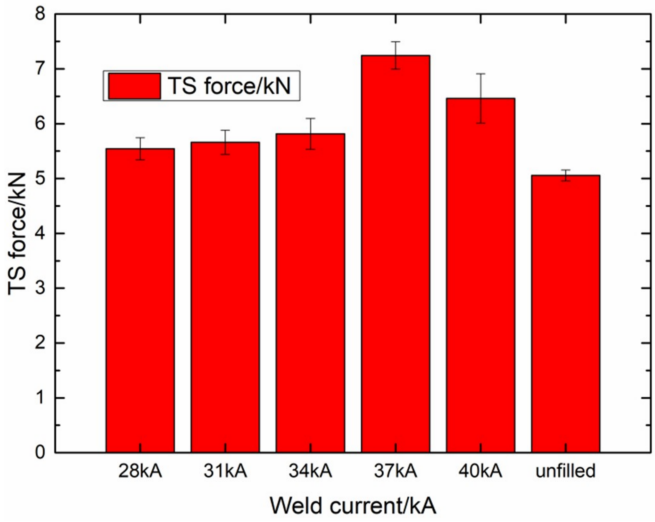

Figure 4. The tensile-shear properties of 2024-T4 aluminum alloy joint with filled/unfilled key-hole, the filling parameter of weld current is 28 kA, 31 kA, 34 kA, 37 kA, and 40 kA respectively.

3.2. Macrostructure

The macrostructure of the keyhole in the unfilled FSSW joint is shown in Figure 5. The joint can be divided into four zones: shoulder affected zone (SAZ), stir zone (SZ), thermo-mechanically affected zone (TMAZ), and heat affected zone (HAZ), respectively. The SAZ in the top sheet is thinned by shoulder of welding tool. In the central section, the SZ encloses the keyhole. Most sections of TMAZ are in the bottom sheet. The section around the SAZ and TMAZ is HAZ. In the joint, the areas of SZ and TMAZ are larger than others, which correlates to the long holding time at high temperatures. In the boundary of the top and bottom sheet, the hook is observed but disappears in the SAZ. On the surface of the keyhole, grooves are seen, which were generated by the thread of the probe of the welding tool. Note that the grooves would increase the contact resistance for keyhole refill using RSW in the present study.

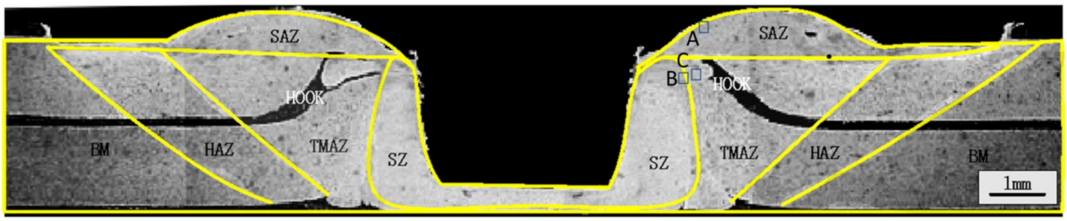

Figure 5. The macrostructure of the FSSW joint with unfilled keyhole.

In comparison, the macrostructure of the cross section of the joint with refilled keyhole is shown in Figure 6. From Figure 6, it is seen that the FSSW keyhole has been filled up, the grooves and the hook are all disappeared. To help understand better the macrostructure, similar to the unfilled FSSW, the following zones in the joint are defined: the fusion welding zone (FWZ), the pressure welding zone (PWZ), the plastic deformation zone (PDZ), and the melted plug zone (MPZ), as illustrated in Figure 6.

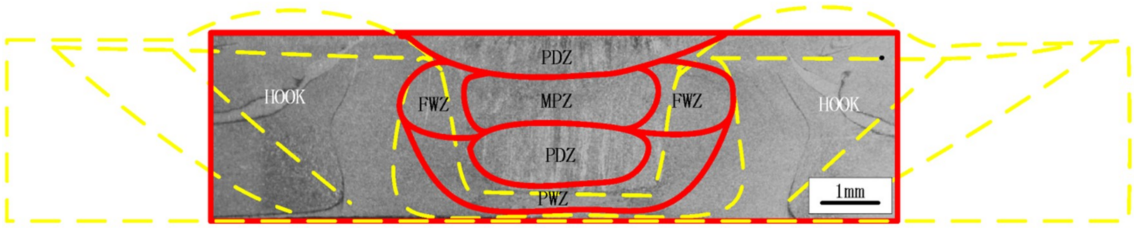

Figure 6. The macrostructure of the joint with filled keyhole.

After the refilling, the SZ of FSSW joint have changed, and the TMAZ and HAZ have not changed, but the gap of hook has be filled and the SAZ has be planished. The hook zone and the SAZ are negative to TS force of joint. The FWZ refers to the area where a fusion joining is formed between the bore of the plug and that of the keyhole. The fusion joining is formed due to primarily two reasons: first, because the welding pressure is perpendicular to the bottom surface of the plug and the bottom surface of the keyhole, the pressure of the FWZ is the most sufficient, the condition of the contact surface is good, and the contact resistance is minimized; and second, because the FWZ is within the shortest movement channel of the charges between the upper and lower electrodes, most welding current primarily flows through this region. The FWZ is limited to the bore of the keyhole, which has a relatively small area. At the early stage of charging for refill, a fusion joining occurs immediately, the contact resistance disappears instantly, and the boundary of the plug and the keyhole undergo metallurgical bonding, which forms a good movement channel of the current and heat. By adjusting the processing parameters and the shape of the plug, the formation time of the FWZ could be precisely controlled, which is the key point in performing keyhole refill using the resistance heat.

The PWZ refers to the zone that the plug is joined to the bore of the keyhole other than the FWZ. The joining was made through a diffusion process. Since the material of the plug is aluminum alloy, its bulk resistance is far smaller than the contact resistance of the binding surfaces, the welding current that flows through the contact surface is extremely small leading the energy of atom diffusion to primarily be due to the heat generated by the bulk resistance of the plug in addition to the interfacial energy generated by the plug and the keyhole during the diffusion process under the lateral pressure of the electrode. Since the efficiency of solid state welding is far less than that of resistance welding, the PWZ forms far later than the FWZ. The difference in forming time between the two helps extrusion of the air between the plug and the keyhole that prevents the generation of the keyhole inside the joint and inclusion of oxides.

The PDZ refers to the zone of the plug that undergoes plastic deformation under the combined effect of electrode pressure and resistance heat, which is found within the area between FWZ and PWZ. The upper portion of the PDZ is sealed by the end of the upper electrode. The PDZ helps the plug

completely refill the keyhole, also lowers the requirement on the shape of the plug and the alignment between the plug and the keyhole.

The MPZ is often found in the middle portion of the plug within the PDZ and FWZ. When the welding current flows through the plug, the bulk resistance generates a large amount of heat rapidly, which cannot be dissipated timely via the electrodes, such that the temperature of the middle portion of the plug increases dramatically leading the temperature of the middle portion of the plug exceeds the melting point. Under the condition that the heat needed by the PWZ is sufficient, by adjusting the processing parameters and the shape of the plug, MPZ may be decreased or even disappear, which promotes the keyhole refill quality.

3.3. Microstructure

Figure 7 shows the microstructure of the FSSW with unfilled keyhole, which are made three marks in Figure 5 (zones A, B and C) for the zones. The SAZ (Figure 7a) undergo through the high welding thermal cycle and strong mixing, which causes higher local deformation providing grain refinement via dynamic recrystallization [19,20]. The grain refinement is also observed in SZ and TMAZ due to the stirring action (Figure 7b,c). Since region SZ is adjacent to the keyhole, most of the stirring action takes place in this region. The grains in this region are subjected to high plunging action and undergo dynamic recrystallization due to the combined effect of high temperature produced by frictional heat and stirring action. Hence, very fine equiaxed grains are obtained with an average grain size of 10 μm. Grains in the vicinity of tool shoulder are deformed and elongated due to the mechanical stirring of tool and grain refinement is also observed in the TMAZ. The average grain size observed in this region is 15 μm in short axis and 40 μm in long axis.

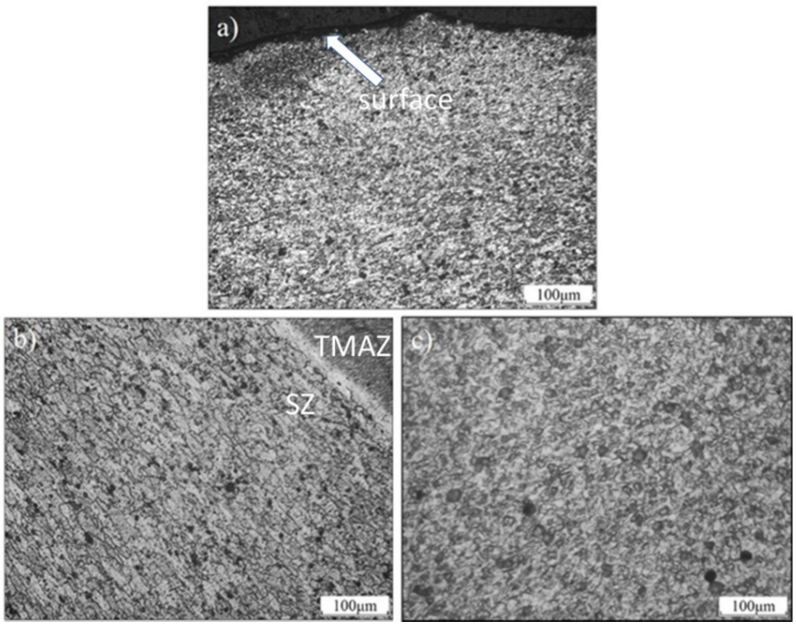

Figure 7. The microstructure of unfilled key-hole: (**a**) shoulder affected zone (SAZ), (**b**) stir zone (SZ), and (**c**) thermo-mechanically affected zone (TMAZ).

Figure 8 shows the microstructure of the refilled FSSW specimen which was welded with the welding current of 37 kA. As shown in Figure 8a, the grains in FWZ mainly include tiny isometric grains and columnar grains, where the diameter of the former ones is approximately 8 μm, and the diameter of the cross-section of the latter one is approximately 18 μm. In the PDZ of the plug above the FWZ as indicated by the arrow in Figure 8a, the grains tilt, and the morphology of the grains on the side area of the keyhole inherits the genes from the columnar grains of this region. Furthermore, the growth direction of the grains is from the plug to the keyhole. The tiny isometric grains are formed by

directional solidification originated from the recrystallized grains at the bottom of the keyhole serving as the nucleation cell towards the plug. The variation in the grain morphology of the original grains in the plug indicate that, during the refill process, the thickness of the melted layer at the bottom of the keyhole is greater than the end portion of the plug. The reason is that, after being polished prior to welding, the surface roughness of the end of the plug is lower than that at the bottom of the keyhole, the current density distribution on the keyhole side is uneven which results in rapid increase in local temperature at the contact surfaces thus the fusion depth being greater than the end portion of the plug. The more improvement in surface finish of the bottom of the keyhole, the more decrease in the contact resistance between the bottom of the keyhole and the plug, and longer formation time of the FWZ. All these help increase the temperature at the PWZ, thus create beneficial conditions to ensure the overall refill quality of the keyhole.

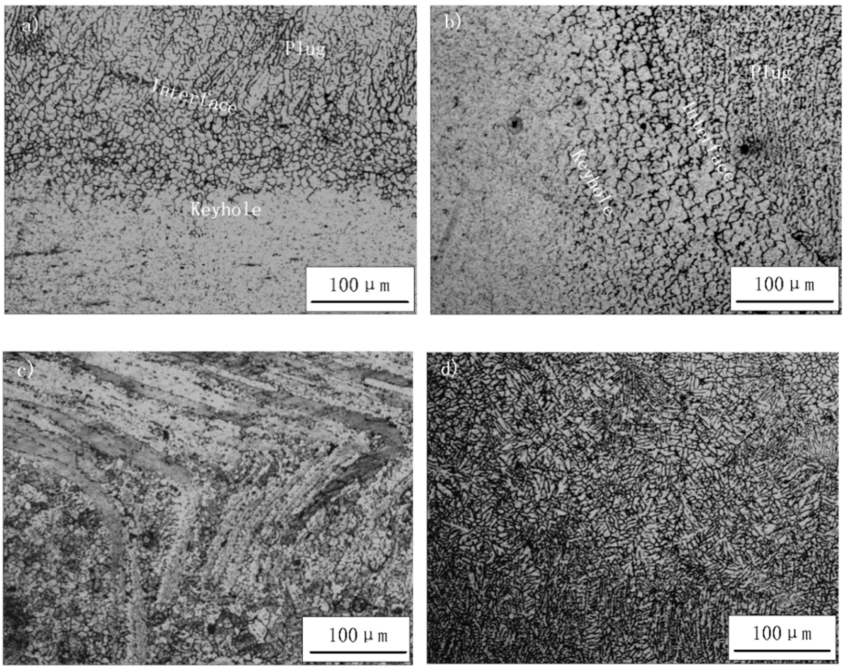

Figure 8. The microstructure of filled key-hole: (**a**) fusion welding zone (FWZ), (**b**) the pressure welding zone (PWZ), (**c**) the plastic deformation zone (PDZ), and (**d**) the melted plug zone (MPZ).

In the PWZ (Figure 8b) which is solid state welding in nature, there is significant differences in grain sizes and grain orientations. Further, self-diffusion is the primary form of the transportation of the metallic atoms. During the refill process, the increased surface energy provides a driving force for the diffusion of the metallic atoms. When the grain boundary moves, the metallic atoms evolve from small grains on the side of the plug into the large grains on the wall of the keyhole leading to larger grains taking over the small grains. When the keyhole refill process completes, the columnar grains in the PDZ on the plug are squeezed and deformed, the number of large grains on the wall of the keyhole increases significantly, and, other than partial large isometric grains being formed by recrystallization of the grains, the large columnar grains close to the contact interface are mainly formed by occupying the small grains of the plug. When the plug has sufficiently high hardness, the electrode pressure is usually effectively transferred), longer time the PWZ at the high temperature increases the thickness of the diffusion layer and enhances the uniformity of the diffusion layer, thus ensures overall quality for the keyhole refill.

As shown in Figure 8c, in the PDZ located in the upper portion of the plug, the original rolled fiber structures show curved and deformed "geometric softening" under the influence of the electrode pressure, where a boundary line (indicated by the dashed line in Figure 8c is applied to connect the bent inflection points. The region above the boundary line primarily shows the recovery phenomenon.

The region below the boundary line shows both the recovery and recrystallization phenomena. The recrystallization region is larger, but the grains in this region are mainly tiny isometric grains. This indicates that with increasing distance from the plug to the central portion of the upper electrode, the temperature of the plug increases gradually due to the bulk resistance heating. Since the drawing aluminum bar was selected as the raw material for the plug, the residual deformation would delay recovery and recrystallization of the plug along the sheet surface where the keyhole is, thus the mechanical performance of the plug is expected to maintain.

The microstructure of the MPZ (Figure 8d) mainly consists of equiaxed dendrites. During the refill process, the heat accumulates in the middle portion of the plug leading to the occurrence of the liquid-phase solidification structures. Furthermore, no original microstructures of the plug are found. Because the middle portion has the poorest heat-dissipation capability, the liquid-phase region or solid-liquid co-existence region must appear in the middle portion of the plug. To prevent the occurrence of crystallization cracks under the effect of the grain shrinkage stress during the crystallization process of the liquid-phase metal, a sufficiently large pressure must be applied to the electrode.

3.4. Microhardness

The microhardness profiles of the unfilled FSSW and filled FSSW specimens made at welding current of 37 kA are presented in Figure 9. From Figure 9, it is seen that in unfilled FSSW specimens, hardness in SZ is the highest, gradually decreases through TMAZ, reaches a minimum value, and finally increases again towards base material. The region with the minimum hardness is identified as HAZ. The region between TMAZ and HAZ is the softest region. The decrease in hardness in HAZ is due to an overaging effect that coarsens the precipitates. SZ is associated with very high temperature and severe plastic deformation. Large precipitates at such high temperatures are dissolved and very fine precipitates form. Thus hardness increase in SZ is mainly due to the fine grains and precipitates. In the refilled FSSW specimens, a similar hardness profile is found. Because of the corona bonding, the hardness of TMAZ and HAZ of the refilled FSSW specimens is higher than that of unfilled FSSW samples. However, it is also noted that the plug in MPZ of hardness is very low, as the region is the melted zone pertaining to an as-cast microstructure.

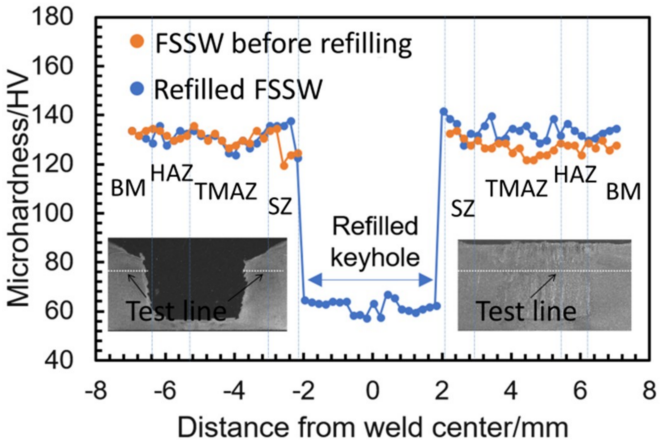

Figure 9. The microhardness profiles of FSSW before and after refill.

3.5. Fracture Behavior

Figure 10 shows fracture in an unfilled FSSW specimen. Figure 10a reveals the macroscopic fracture surface of the close-up top view the bottom sheet. It is seen in Figure 10a that pull-out fracture occurs along the hook nearly the boundary between the top and bottom sheets along the periphery of the keyhole. This is more evident in the cross-section view of the fractured specimen

(Figure 10b). Figure 10c–e reveals the magnified views of different locations labeled A, B, and C of the fracture surface in Figure 10c, respectively. In region A, many grooves are observed along the thread of probe of weld tool. It is evident that the region A does not contribute to improving joint TS strength. The fracture surfaces shown in region B of SZ exhibit some elongated dimples of various sizes in the same direction. The crack is initiated in the region C, where the hook is located. In this region, very few dimples are observed where the crack has initiated and propagated along the partially bonded boundary.

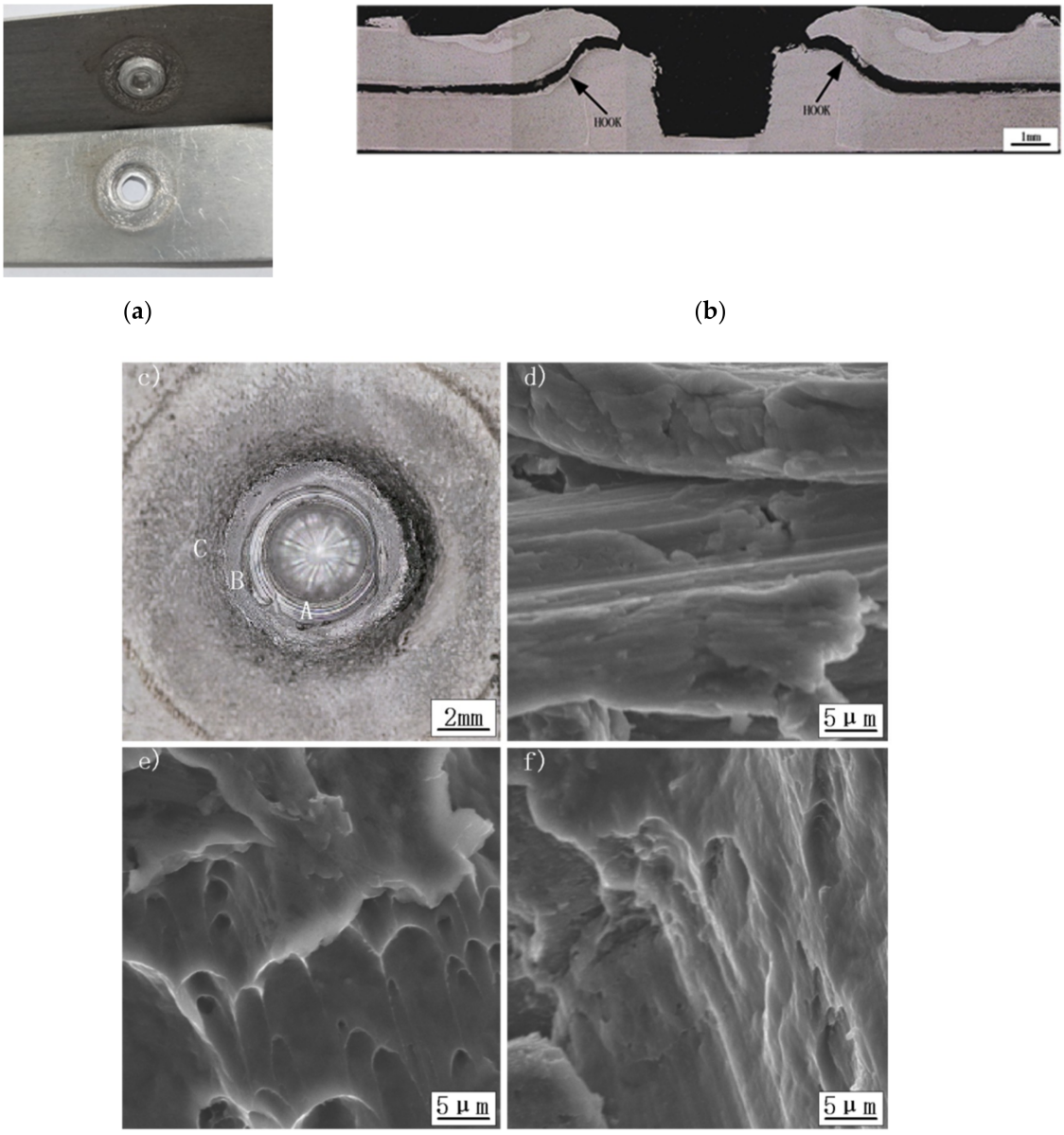

Figure 10. Fracture in unfilled FSSW sample: (**a**) fractured specimen; (**b**) cross section of the fractured specimen; (**c**) SEM images of fracture surface on the bottom sheet; (**d**), (**e**), (**f**) magnified views in the zones A, B, and C in (**c**), respectively.

Figure 11 shows fracture in a refilled FSSW specimen. Figure 11a reveals the macroscopic fracture surface of the close-up top view the bottom sheet showing also pull-out fracture. From the cross-section view of the fracture specimen, it is interesting to note that the fracture occurs in the corona bonding zone (Figure 11b). From the SEM images of fracture surface (Figure 11c), it is seen that the crack is initiated in the region C of corona bond zone which is generated during filled the keyhole by RSW,

where it is the porous zone. In the region, a large number but small dimples are observed where the crack has initiated and propagated along the partially bonded boundary. The fracture surfaces shown in region A of PDZ (Figure 11d) and region B of SZ (Figure 11e) exhibit some elongated dimples of various sizes in the same direction, and the dimples in the region B is deeper than in the region A indicating region B could have better ductility than region A.

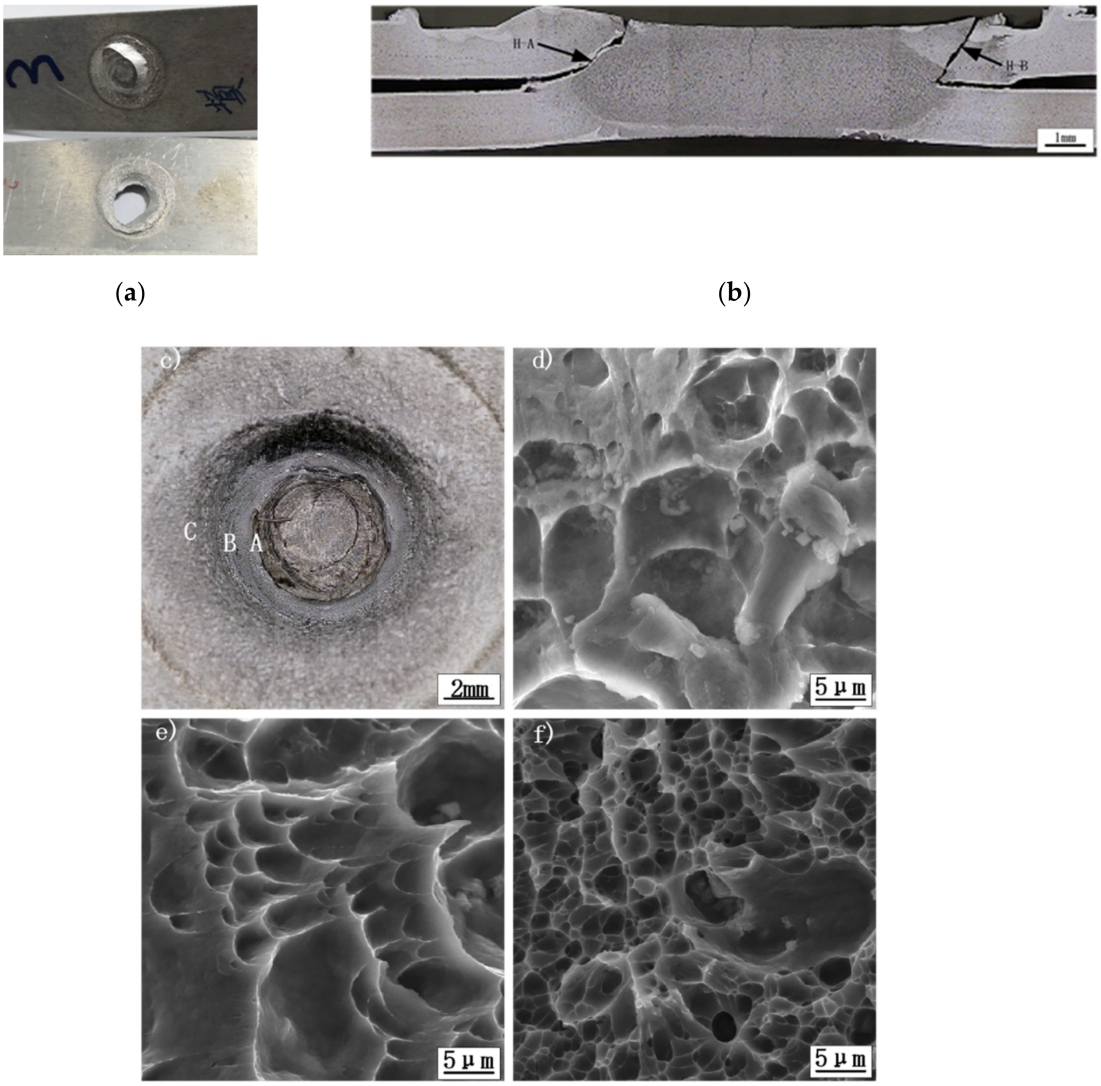

Figure 11. Fracture in refilled FSSW sample by RSW: (**a**) fractured specimen; (**b**) cross section of the fractured specimen; (**c**) SEM images of fracture surface on the bottom sheet; (**d**–**f**) magnified views in the zones A, B, and C in (**c**), respectively.

When comparing fracture locations in the FSSWs with unfilled and refilled holes as shown in Figure 10; Figure 11, it is understood that the increase in static TS force in FSSW refilled with RSW technique is attributed to the absence of keyhole and presence of extra material in the refilled joint caused by corona bonding. This extra material from the corona ring will create more compact pressure, leading to increased bonding area, thus enhancing the static TS force. In the unfilled joints, the keyhole and hook present act as notches during tensile shear testing and cause excessive stress concentration. This led to the initiation and propagation of the crack, leading to poor mechanical properties.

Based on discussions aforementioned, the presence of elongated dimples in fracture surfaces of the unfilled and refilled FSSW specimens indicates the shear fracture occurred at the final stage of failure [21,22], and the refilled specimens has better ductility than the unfilled specimens. This is

consistent with the larger cross head movement displacement as shown in the tensile curves of the refilled FSSW specimens in Figure 4.

4. Conclusions

A novel keyhole refill technique is developed for friction stir spot welding (FSSW) using resistance spot welding (RSW) and is applied successfully to refill a keyhole generated in friction stir spot welded 1.5 mm thick 2024-T4 aluminum alloy sheets. The following conclusions can be drawn.

(1) The filled FSSW joint can be divided as follows: the fusion welding zone (FWZ), the pressure welding zone (PWZ), the plastic deformation zone (PDZ), and the melted plug zone (MPZ). And the shoulder affected zone (SAZ) and hook zone in the unfilled FSSW joint can be removed by the novel refilling technique.

(2) The refill process significantly improved the maximum load capacity in tensile shear testing due to a larger corona bonding area after the refill. In the filled FSSW joint, the TS force first increases and then decreases with increasing welding current with a peak value of 7.25 kN at weld current of 37 kA which is 33% higher than that of the unfilled FSSW joint.

(3) In the filled FSSW joint, the hardness profile is similar to the unfilled joint around the keyhole, but the hardness of plug in keyhole is very low.

(4) The tensile shear fracture occurs in the filled FSSW joint at the corona bonding zone, while the fracture occurs at the hook zone in the unfilled keyhole.

Author Contributions: Funding acquisition, L.K. and L.D.; Investigation, J.K., S.L. and J.L.; Methodology, L.D., J.K. and S.L.; Supervision, L.K. and J.L.; Writing—original draft, L.D.; Writing—review & editing, J.K., S.L., L.K. and J.L.

Funding: The authors acknowledged the financial support from the National Natural Science Foundation of China, grant number 51265043; and from the Jiangxi Education Department Natural Science Foundation, grant number DA201803177.

Conflicts of Interest: The authors declare no conflict of interest.

References

1. Thomas, W.M.; Nicholas, E.D.; Dawes, C.J. Friction stir butt welding. GB 9125978 A, 6 December 1991 and US 5460317 B1, 9 December 1997.
2. Aonuma, M.; Nakata, K. Dissimilar metal joining of 2024 and 7075 aluminium alloys to titanium alloys by friction stir welding. *Mater. Trans.* **2011**, *52*, 948–952. [CrossRef]
3. Cavaliere, P.; Cerri, E.; Squillace, A. Mechanical response of 2024-7075 aluminium alloys joined by friction stir welding. *J. Mater. Sci.* **2005**, *40*, 3669–3676. [CrossRef]
4. Li, Y.; Trillo, E.A.; Murr, L.E. Friction-stir welding of aluminum alloy 2024 to silver. *J. Mater. Sci. Lett.* **2000**, *19*, 1047–1051. [CrossRef]
5. Ding, R.J.; Oelgoetz, P.A. Auto-adjustable pin tool for friction stir welding. US 5893507 A, 13 April 1999.
6. Yang, X.; Fu, T.; Li, W. Friction Stir Spot Welding: A review on joint macro- and microstructure, property and process modelling. *Adv. Mater. Sci. Eng.* **2014**, *2014*, 697170. [CrossRef]
7. Li, W.; Lin, J.; Zhang, Z.; Gao, D.; Wang, W.; Dong, C. Improving mechanical properties of pinless friction stir spot welded joints by eliminating hook defect. *Mater. Des.* **2014**, *62*, 247–254. [CrossRef]
8. Chu, Q.; Li, W.Y.; Yang, X.W.; Shen, J.J.; Vairis, A.; Feng, W.Y.; Wang, W.B. Microstructure and mechanical optimization of probeless friction stir spot welded joint of an Al-Li alloy. *J. Mater. Sci. Technol.* **2018**, *34*, 1739–1746. [CrossRef]
9. Li, W.Y.; Chu, Q.; Yang, X.W.; Shen, J.J.; Vairis, A.; Wang, W.B. Microstructure and morphology evolution of probeless friction stir spot welded joints of aluminum alloy. *J. Mater. Process. Technol.* **2018**, *252*, 69–80. [CrossRef]
10. Riki, T.; Terry, L.K. Friction plug welding. US 6213379 B1, 10 April 2011.
11. Andrews, R.E.; Mitchell, J.S. Underwater repair by friction stitch welding. *Met. Mater.* **1990**, *6*, 796–797.

12. Metz, D.F.; Weishaupt, E.R.; Barkey, M.E.; Fairbee, B.S. A microstructure and microhardness characterization of a friction plug weld in friction stir welded 2195 Al-Li. *J. Eng. Mater. Technol. -Trans. ASME* **2012**, *134*, 1–7. [CrossRef]
13. Metz, D.F.; Barkey, M.E. Fatigue behavior of friction plug welds in 2195 Al-Li alloy. *Int. J. Fatigue* **2012**, *43*, 178–187. [CrossRef]
14. Huang, Y.; Han, B.; Tian, Y.; Liu, H.J.; Lv, S.X.; Feng, J.C.; Leng, G.S.; Li, Y. New technique of filling friction stir welding. *Sci. Technol. Weld. Joining* **2011**, *16*, 497–501. [CrossRef]
15. Wang, G.Q.; Zhao, G.; Hao, Y.F.; Chen, X.F.; Zhao, Y.H. Technology for repairing keyhole defect for FSW joint of 2219 aluminum alloy. *Aerosp. Mater. Technol.* **2012**, *42*, 24–28.
16. Tuatar, M.; Aydin, H.; Bayram, A. Effect of weld current on the microstructure and mechanical properties of resistance spot-welded TWIP steel sheet. *Metals* **2017**, *7*, 519. [CrossRef]
17. Jia, Q.; Liu, L.; Guo, W.; Peng, Y.; Zou, G.S.; Tian, Z.L.; Zhou, Y.N. Microstructure and tensile-shear properties of resistance spot-welded medium Mn steel. *Metals* **2018**, *8*, 48. [CrossRef]
18. Karthikeyan, R.; Balasubramaian, V. Optimization of Electrical Resistance Spot Welding and Comparison with Friction Stir Spot Welding of AA2024-T3 Aluminum Alloy Joints. *Mater. Today Proc.* **2017**, *4*, 1762–1771. [CrossRef]
19. Etter, L.; Baudin, T.; Fredj, N. Recrystallization mechanisms in 5251-H14 and 5251-O aluminum friction stir welds. *Mater. Sci. Eng. A* **2007**, *445–446*, 94–99. [CrossRef]
20. Mcnelley, T.R.; Swaminathan, S.; Su, J. Recrystallization mechanisms during friction stir welding/processing of aluminum alloys. *Scr. Mater.* **2008**, *58*, 349–354. [CrossRef]
21. Shen, Z.; Yang, X.; Zhang, Z.; Cui, L.; Li, T. Microstructure and failure mechanisms of refill friction stir spot welded 7075-T6 aluminum alloy joints. *Mater. Des.* **2013**, *44*, 476–486. [CrossRef]
22. Zhang, Z.; Yang, X.; Zhang, J.; Zhou, G.; Xu, X.; Zou, B. Effect of welding parameters on microstructure and mechanical properties of friction stir spot welded 5052 aluminum alloy. *Mater. Des.* **2011**, *32*, 4461–4470. [CrossRef]